REVIEW OF BIFURCATIONS IN YANG–MILLS MECHANICS*

J. KARKOWSKI

Institute of Physics, Jagellonian University
Reymonta 4, 30-059 Cracow, Poland

(Received July 7, 1990; revised version received October 24, 1990)

Classical Yang–Mills mechanics is shortly reviewed. The family of basic periodic orbits corresponding to different values of energy was found. Several unstable bifurcations existing in this family are presented in detail and compared with their counterparts from the ZOO of stable bifurcations. A brief discussion of the separatrix splitting is also included.

PACS numbers: 03.50.Kk

Introduction

The Yang–Mills (Y–M) mechanics is the dynamical system arising as the Y–M potentials in the whole Y–M gauge theory are assumed to be time dependent only. Of course the resulting equations of motion strongly depend on a chosen gauge group and a fixed gauge. We have limited ourselves to the SU(2) gauge group and the simplest gauge choice. Thus we have obtained the one-parameter system of Hamiltonian equations in four dimensional phase-space. This dynamical system was extensively studied for the special value of the above mentioned parameter. The theory arising then is claimed to be chaotic [1]. Any other possible choice of the parameter gives rise to a completely different system, exhibiting weak chaotic behaviour only [2] It turns out however that this system is also interesting from the other point of view. Namely: a family of unstable bifurcations can be observed very clearly using rather simple numerical procedures. All (stable) bifurcations in four dimensional Hamiltonian systems are described in detail [3]. However from the physical point of view unstable bifurcations are more interesting

* This work was supported by Polish Ministry of Education, Project CPBP 01.03.1.7.

as they are closely related to the symmetry properties of the system under study. This is our motivation to present them and compare with their stable counterparts.

The paper is organized as follows: Sect. 1 presents the Y–M dynamical system and (shortly) the numerical algorithms used in our analysis. In Sect. 2 the family of basic, periodic orbits (dependent on energy E) is studied in detail. The route of the PCM (principal characteristic multiplier) on the complex plane is particularly interesting. Sect. 3 presents graphically the (unstable) bifurcations existing in the above mentioned family of trajectories. We also compare them with the appropriate members of ZOO of stable bifurcations. The last Section involves the (short) description of the so-called separatrix splitting which can be observed in our model.

1. Yang–Mills mechanics

We regard Y–M mechanics as the dynamical system corresponding to the SU(2) gauge theory with the simplest possible gauge choice [1]. This system is governed by the following set of Lagrangian type differential equations:

$$\begin{aligned} \ddot{s} &= -\dot{w}(\dot{s}w - u\dot{z}), \\ \ddot{z} &= \dot{u}(\dot{s}w - u\dot{z}), \\ \ddot{u} &= \dot{z}(\dot{s}\dot{w} - uz), \\ \ddot{w} &= -\dot{s}(\dot{s}w - u\dot{z}); \end{aligned} \tag{1.1}$$

subject to the kinematical constraint:

$$s\dot{z} - \dot{s}z + u\dot{w} - \dot{u}w = 0. \tag{1.2}$$

(A dot over a letter denotes the differentiation with respect to time.) It can easily be checked that

$$\begin{aligned} L_1 &= (s + w)(\dot{u} - \dot{z}) - (\dot{s} + \dot{w})(u - z), \\ L_2 &= (s - w)(\dot{u} + \dot{z}) - (\dot{s} - \dot{w})(u + z), \end{aligned} \tag{1.3}$$

are constants of motion of the Eqs (1.1) and the constraint (1.2) requires the equality $L_1 = L_2$. Taking this into account we can reduce Eqs (1.1) and (1.2) to the two dimensional Hamiltonian system with

$$\mathcal{H} = \tfrac{1}{2}(p_x^2 + p_y^2) + \tfrac{1}{2}x^2y^2 + L^2\frac{x^2+y^2}{(x^2-y^2)^2}, \tag{1.4}$$

where

$$x^2 = \tfrac{1}{2}\left((s+w)^2 + (u-z)^2\right),$$
$$y^2 = \tfrac{1}{2}\left((s-w)^2 + (u+z)^2\right),$$
$$p_x = \dot{x},$$
$$p_y = \dot{y}. \tag{1.5}$$

and $L \equiv L_1 = L_2$. This system with $L = 0$ was extensively studied and is claimed to be chaotic [1]. Its qualitative behaviour for $L \neq 0$ weakly depends on the definite value of L and we limit ourselves to the simple choice $L^2 = 0.5$. The Hamiltonian (1.4) is singular for $|x| = |y|$ and thus the (x, y)-plane is divided into four disconnected parts. Our investigations are limited to the region $x \geq |y|$ but because of the symmetries $x \leftrightarrows y$ and $x \to -x$, $y \to -y$ any other choice will lead to the same results. The motion of the system has an oscillating character both in x and y directions apart from the only solution for which $y(t) \equiv 0$ [2]. We exclude it from further considerations as our aim is to study periodic solutions and their bifurcations. This allows us to reduce the whole system to the two first order (non-Hamiltonian) differential equations with the phase of y-direction oscillations as the new independent variable. It is important to note that this reduction has a global character and is valid on the whole phase space. To be more precise: we define the action-angle type variables:

$$y = \sqrt{\frac{2I}{x}} \sin\varphi,$$
$$p_y = \sqrt{2Ix} \cos\varphi. \tag{1.6}$$

It can easily be proved that $\dot{\varphi} > 0$ what justifies our choice of the independent variable. The variable I is calculated from the energy formula as a function of x, p_x, φ, the energy E and the parameter L. Finally we obtain the following set of differential equations [2]:

$$\frac{dx}{d\varphi} = \frac{py}{m(\varphi, x, p; E, L)},$$
$$\frac{dp}{d\varphi} = \frac{l(\varphi, x, p; E, L)}{m(\varphi, x, p; E, L)}, \tag{1.7}$$

where $p \equiv p_x$, $v \equiv 1/x$ and the (rather complicated) formulas for the functions l and m are given below:

$$l(\varphi, x, p; E, L) = -x^2 z + 2L^2 v^4 \frac{1+3z}{(1-z)^3},$$

$$m(\varphi, x, p; E, L) = 1 + pv^2 \sin\varphi \cos\varphi + b\frac{3+z}{(1-z)^3}, \tag{1.8}$$

with:

$$\begin{aligned}
b &= 2L^2 v^6 \sin^2\varphi, \\
z &= \begin{cases} \frac{1}{3}a + \frac{1}{3}(2 - d_1 - d_2), & \text{if } \Delta \geq 0; \\ \frac{1}{3}a + \frac{2}{3}\left(1 + c\sqrt{(1-a)^2 - 3b}\right), & \text{if } \Delta < 0; \end{cases} \\
a &= \left(2E - p^2\right) v^4 \sin^2\varphi, \\
d_1 &= \sqrt[3]{(1-a)^3 + \tfrac{9}{2}(5+a) + 9\sqrt{\Delta}}, \\
d_2 &= \sqrt[3]{(1-a)^3 + \tfrac{9}{2}(5+a) - 9\sqrt{\Delta}}, \\
\Delta &= \tfrac{1}{3}b^3 + b^2\left(\tfrac{1}{4}(5+a)^2 - \tfrac{1}{3}(1-a)^2\right) + \tfrac{2}{3}b(1-a)^3, \\
c &= \min(\cos\psi_1, \cos\psi_2, \cos\psi_3), \\
\psi_1 &= \tfrac{\psi}{3}; \quad \psi_2 = \tfrac{\psi}{3} + \tfrac{2\pi}{3}; \quad \psi_3 = \tfrac{\psi}{3} - \tfrac{2\pi}{3}, \\
\psi &= \arccos\left(\frac{-(1-a)^3 - \frac{9}{2}ba^2}{\left((1-a)^2 - 3b\right)^{\frac{3}{2}}}\right).
\end{aligned} \tag{1.9}$$

The system (1.7) is very suitable for numerical calculations because it ensures that the obtained (numerical) solutions remain strictly on the constant energy surface. Our numerical analysis is based on several algorithms: the fifth order Runge–Kutta method with adaptive stepsize control [4], the Bulirsch-Stoer method with the Richardson extrapolation [4] and the Gear's algorithm for stiff differential equations [5].

2. The family of periodic orbits

We have found the one parameter family of periodic orbits of the system (1.4). The parameter is the energy E which varies between 0.1 and 100.0. (The other parameter — as was mentioned in the previous Section — is fixed: $L^2 = 0.5$.) The orbits of our family are basic in the sense that they consist of only one oscillation in the y direction. Fig. 1 presents a view of a typical trajectory in the (x, y)-plane on the background of the equipotential lines of the potential given in (1.4). For each periodic orbit Γ from the family we regard the Poincaré mapping $\mathcal{P}$ [3] on the local transversal section $\mathcal{S}$ of Γ defined by the condition $y = 0$ and restricted to the constant energy surface Σ_E. $\mathcal{S}$ may be described by the pair of coordinates $(x, p \equiv p_x)$. Γ corresponds of course to the fixed point of $\mathcal{P}$. According to the symplectic eigenvalue theorem the characteristic multipliers of $\mathcal{P}$ are λ and λ^{-1} (for

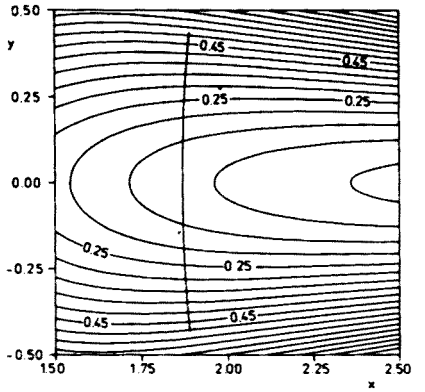

Fig. 1. A typical periodic orbit on the background of equipotential lines ($E = 0.5$).

complex λ the equality $|\lambda| = 1$ must also be fulfilled). In practice we obtain λ regarding the system (1.7) linearized in the neighborhood of Γ. The so-called principal characteristic multiplier (PCM) [3] is defined as that λ for which $|\lambda| > 1$ in the real case or $\mathrm{Im}\,\lambda > 0$ in the complex case. The PCM moves on the complex plane with varying energy. Its route (see Fig. 2) gives

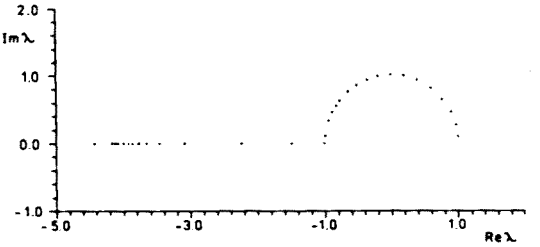

Fig. 2. The route of the PCM on the complex plane ($E_{\min} = 0.1$, $E_{\max} = 100.0$).

us an important qualitative information about the system under study. The fixed point of $\mathcal{P}$ is called elliptic if the appropriate PCM satisfies: $|\lambda| = 1$ and hyperbolic if $|\lambda| > 1$. This terminology becomes obvious when we compare the two phase portraits on the Section $\mathcal{S}$ corresponding to both just mentioned cases (Fig. 3). Loosely speaking the dynamical system in the neighborhood of elliptic Γ is integrable and chaotic if Γ is hyperbolic.

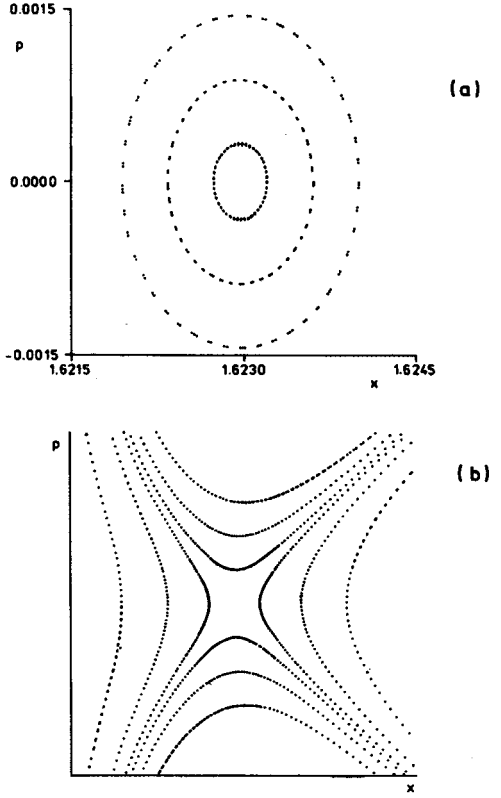

Fig. 3. The neighborhood of the fixed point of $\mathcal{P}$: (a) elliptic case ($E = 1.0$), (b) hyperbolic case ($E = 1.51$).

3. Review of bifurcations

It can easily be checked that Hamiltonian (1.4) has no critical points. Therefore possible bifurcations existing in our dynamical system must be connected with its periodic solutions [3]. In this Section we present several bifurcations we have found in the family of the basic periodic orbits described in Sect. 2. Each bifurcation of a given trajectory corresponds of course to the bifurcation of a appropriate fixed point of the Poincaré mapping $\mathcal{P}$ introduced earlier. Fig. 2 suggests that the PCM acquires (for our periodic solutions) all complex values on the unit circle in the upper half plane. The possible (stable) bifurcations in such case are classified and may be the following ones: emission (absorption), phantom kiss and subtle division (murder) [3]. However our system possesses the symmetry: $y \to -y$ mentioned in Sect. 1. This symmetry may be easily broken by many different perturbations and therefore the Hamiltonian (1.4) is not structurally

stable. That is why it seems interesting to compare bifurcations existing in our model with their stable counterparts. We expect the periodic trajectories of our family to bifurcate when the PCM takes the value $\exp(i2\pi/n)$ with $n = 2, 3, \ldots$ ($n = 1$ is excluded because for $E \to 0$ the PCM tends to but never reaches 1.0). Let us begin with $n = 5$. The emission of two trajectories then occurs (Fig. 4). One of them is elliptic and the other hyperbolic.

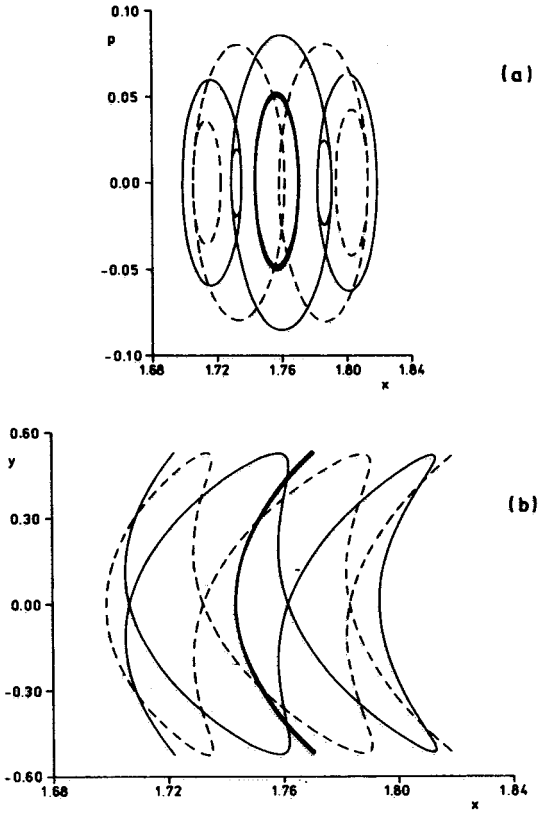

Fig. 4. The emission of two orbits: elliptic (solid) and hyperbolic (dashed); ($n = 5$, $E = 0.64$, PCM = $\exp(0.40104\Pi i)$): (a) (x, p) view, (b) (x, y) view.

Their periods are five times greater than the appropriate basic ones (as in the stable case). The cases with $n = 3, 4$ are similar. The phantom kiss is not observed. Instead the emission of two orbits (elliptic and hyperbolic) takes place as for $n = 5$. When $n = 3$ (Fig. 5) the new periods are thrice as much as the basic periods. The case $n = 4$ differs in this respect however, because the periods of the new orbits are only doubled (Fig. 6). The similar situation occurs for $n = 2$. The transition of the basic trajectory from elliptic to hyperbolic is accompanied by the emission of the (elliptic) orbit

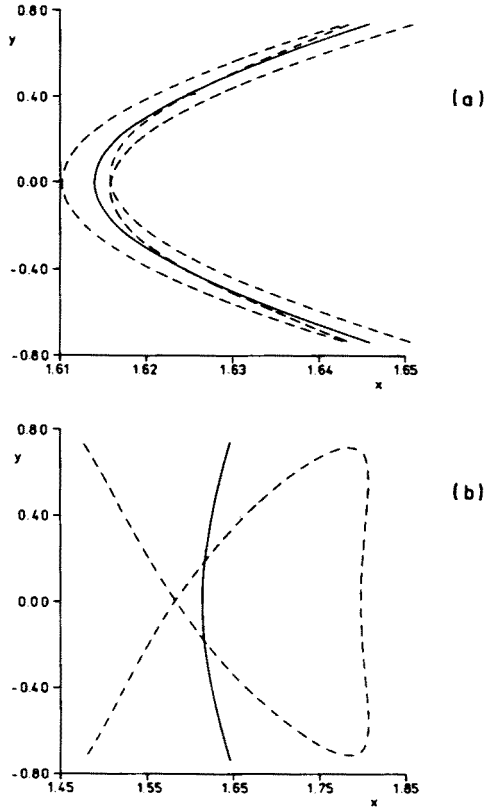

Fig. 5. The basic period trajectory (solid) with the emitted one (dashed); ($n = 3$, $E = 1.083$, PCM = exp(0.66806IIi): (a) of hyperbolic type, (b) of elliptic type.

with the same period (Fig. 7). This bifurcation resembles the (stable) subtle division but then the new period is doubled. In general case n odd the emission takes place identical with that of the stable case. When n is even the situation differs because the periods of the new orbits are twice less as expected for stable bifurcations. The above mentioned symmetry $y \to -y$ is responsible for this fact (compare [6]). The basic trajectories are invariant under this symmetry and posses two turning rest points. Therefore their projections on the (x, p)-plane wind twice the same route during each period. The similar situation occurs for bifurcations with n odd. For n even however, the new trajectories are either non-invariant under the existing symmetry or do not posses turning rest points. Therefore they follow only once their route on the (x, p)-plane during each period. From the other side the Poincaré section $\mathcal{S}$ (defined by $y = 0$) is obviously invariant under $y \to -y$ and the fixed points of the Poincaré mapping $\mathcal{P}$ are reached twice a

period for orbits of the first type and once for the trajectories of the second type. These are the sources of the described complications.

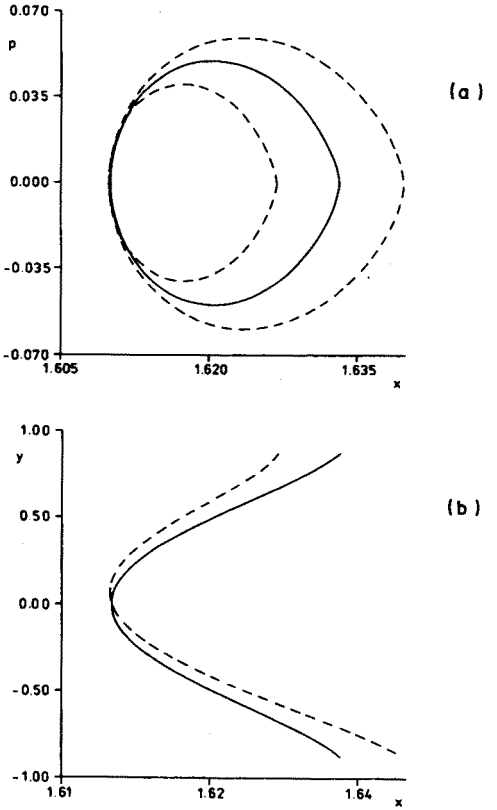

Fig. 6. The emission of new trajectories ($n = 4$, $E = 1.505$, PCM = $\exp(0.50002\Pi i)$): (a) elliptic one, (b) hyperbolic one.

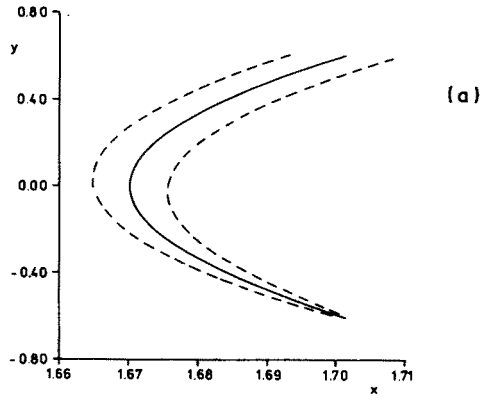

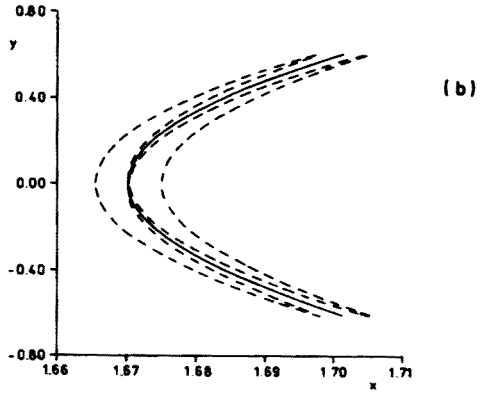

Fig. 7. The (unstable) subtle division. The basic trajectory (solid) and the emitted (dashed) elliptic one ($n = 2$, $E = 1.505$, PCM $= 1.02417$): (a) (x, p) view, (b) (x, y) view.

4. Separatrix splitting

In the foregoing Section we have described two types of bifurcations existing in our model: the subtle division ($n = 2$) and the emission ($n = 3, 4, 5$). When the emission takes place two new periodic orbits appear: one elliptic and the other hyperbolic. This type of bifurcation is closely connected with the so-called separatrix splitting: an important and hardly understood reality accompanying the transition from integrable to chaotic region [7]. We briefly present how it happens limiting ourselves to $n = 3$. Let E_0 be the value of our main parameter (*i.e.* energy) for which the emission (with $n = 3$) occurs. When $E > E_0$ and the difference $E - E_0$ is small the three points at which the (emitted) hyperbolic orbit intersects the Poincaré Section $\mathcal{S}$ are very close to the fixed point corresponding to the basic periodic trajectory. The sides of the triangle assigned by these three points (together with their extensions) from the figure (called separatrix) invariant under the Poincaré mapping $\mathcal{P}$ (Fig. 8). The separatrix divides $\mathcal{S}$ into disconnected parts which can be grouped into three subareas also invariant under $\mathcal{P}$.

This picture is nearly the same as that corresponding to the linearized equations in the neighborhood of the given periodic orbit. For E much greater than E_0 however, the separatrix splits into six very complicated curves crossing each other and filling the section $\mathcal{S}$. The invariant subregions of $\mathcal{S}$ seem not to exist any more. Numerical computations give a picture like that on Fig. 9. It is impossible of course to calculate strictly the value of E for which the separatrix splitting begins and what is the shape of the splitted lines.

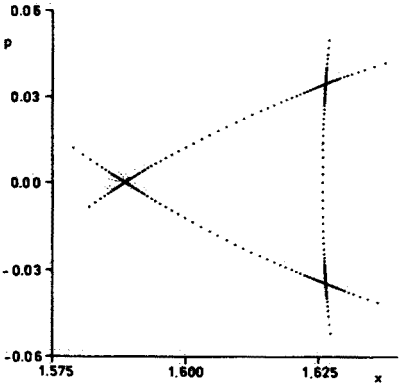

Fig. 8. The numerical picture of the separatrix near the bifurcation energy value ($n = 3$, $E = 1.1$).

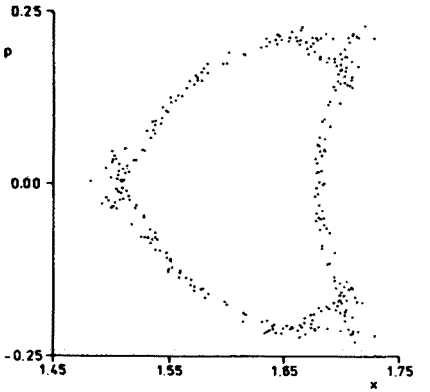

Fig. 9. The splitted separatrix ($n = 3$) for the energy far from its bifurcation value ($E = 1.3$).

REFERENCES

[1] S.G. Matinyan, G.K. Savvidi, N.G. Ter-Arutyunyan, *Zh. Eksp. Teor. Fiz.* **80**, 830 (1981); I. Fröland, *Phys. Rev.* **D27**, 943 (1983).

[2] J. Karkowski, *Acta Phys. Pol.* **B21**, 529 (1990).

[3] R. Abraham, J.E. Marsden, *Foundations of Mechanics*, The Benjamin/Cummings Publishing Company, Inc. 1978, Chapter 8.

[4] W.H. Press, B.P. Flannery, S.A. Teukolsky, W.T. Vetterling, *Numerical Recipes, The Art of Scientific Computing*, Cambridge University Press, 1987, Chapter 15.

[5] C.W. Gear, *Comm. ACM* **14**, 185 (1971).

[6] M.A.M. De Aguilar, C.P. Malta, *Physica* **30D**, 413 (1988).

[7] V.I. Arnold, *Mathematical Methods of Classical Mechanics*, MIR, Moskva 1975, Appendix 7.